Applied Clay Science 253 (2024) 107350

Contents lists available at ScienceDirect

Applied Clay Science

journal homepage: www.elsevier.com/locate/clay

Research Paper

Sicilian clay sediments as precursor for alkali activated materials

Antonio Stroscio [a], Germana Barone [a], Ana Fernàndez-Jimenez [b], Isabella Lancellotti [c], Cristina Leonelli [c], Paolo Mazzoleni [a,*]

[a] University of Catania, Department of Biological, Geological and Environmental Science, Catania, Italy
[b] Eduardo Torroja Institute (CSIC), c/Serrano Galvache, n 84, 28080 Madrid, Spain
[c] University of Modena and Reggio Emilia, Department of Engineering "Enzo Ferrari", Modena, Italy

ARTICLE INFO

Keywords:
Clay sediment
AAMs (with and without lime)
Eco-friendly binders
Sicily

ABSTRACT

In this work, we focused on the possibility of using clay sediments found in Sicily as precursors to produce alkali activated materials (AAMs) with properties comparable to those of traditional materials used in construction. Two different clays were selected: Plio-Pleistocenic marly clay (PP) and Numidian Flysh clay (NU) to test the use of sediments with and without calcite. AAMs were prepared using precursors thermally treated at 700 °C and alkaline activator solutions as NaOH 4, 6 and 8 M with or without sodium silicate. All samples were cured at 85 °C for 20 h and at room temperature for 28d. Mineralogical analyses, FTIR data, SEM/EDS morphological and chemical observations showed the formation of a polycondensed gel after 20 h. AAMs obtained from calcite-rich clayey sediments (thermally treated) achieved good compressive strength after 28 days with all activators. However, AAMs based on thermally treated calcite-free clays only showed good compressive strength development only when activated with 8 M NaOH and sodium silicate.

1. Introduction

Since the last decade, the awareness of ecological issues and in particular the problems of CO_2 emissions and of the exploitation of the geological resources, has determined a growing interest in the scientific community for the new class of materials commonly known as Alkali Activated Materials (AAMs) (Benito et al., 2013). These innovative materials are prepared starting from one or more solid aluminosilicate precursors and a liquid alkaline activator solution, usually composed of an alkaline metal hydroxide (typically NaOH or KOH), often accompanied by sodium silicate (Davidovits, 1991). The reactions between the solid and liquid components described in the literature take place in simultaneous stages: dissolution, gelation, reorganization and polymerization (Davidovits, 1991; Fernández-Jiménez and Palomo, 2009). The final properties of the AAMs depend on several factors (Pacheco--Torgal et al., 2008): i) chemical composition of the precursors; ii) reactivity of the solid phases; iii) pH value and composition of the activation solution; iv) solid/liquid ratio; v) curing conditions. The excellent physico-mechanical properties of AAM's allow their use as new construction materials with lower environmental impact compared to Ordinary Portland Cement (OPC), (Van Deventer et al., 2010; Juenger et al., 2011; Provis, 2018). In addition, AAMs exhibit high durability, low shrinkage, low thermal conductivity, and good resistance to fire and various acids and salt solutions (Schmücker and MacKenzie, 2005). The most common precursors are solid industrial residues or wastes such as fly ash, metallurgical slags, mining wastes, or industrial minerals such as kaolinite or feldspars, which ensure high performance of AAMs (Oh et al., 2014; Wang et al., 2021; Liang et al., 2022; Kang et al., 2023; Wang et al., 2023b). Recently, several natural materials, such as volcanic ash (Occhipinti et al., 2020) and clayey sediments (Barone et al., 2020; Tchakouté et al., 2020; Christophliemk et al., 2022; Vasic et al., 2022; Žibret et al., 2023), have shown good performance due to their chemical composition ($Al_2O_3 + SiO_2 > 70\%$) and high reactivity in alkaline environments. Nowadays, the development of "just add water" one-part alkali-activated materials (OP-AAM) has attracted much attention, mainly due to their advantages in overcoming the hazardous, irritating, and corrosive nature of activator solutions, (Qin et al., 2022). As it is known, clay minerals are an abundant and diverse source of aluminosilicates available worldwide. However, their use has been more limited due to the mineralogical complexity of the most common clay minerals such as kaolinite, halloysite, montmorillonite and illite, and practical issues such as workability. Recent advances have improved the

* Corresponding author.
E-mail addresses: antonio.stroscio@phd.unict.it (A. Stroscio), germana.barone@unict.it (G. Barone), anafj@ietcc.csic.es (A. Fernàndez-Jimenez), isabella.lancelotti@unimore.it (I. Lancellotti), cristina.leonelli@unimore.it (C. Leonelli), paolo.mazzoleni@unict.it (P. Mazzoleni).

https://doi.org/10.1016/j.clay.2024.107350
Received 30 November 2023; Received in revised form 21 March 2024; Accepted 24 March 2024
Available online 28 March 2024

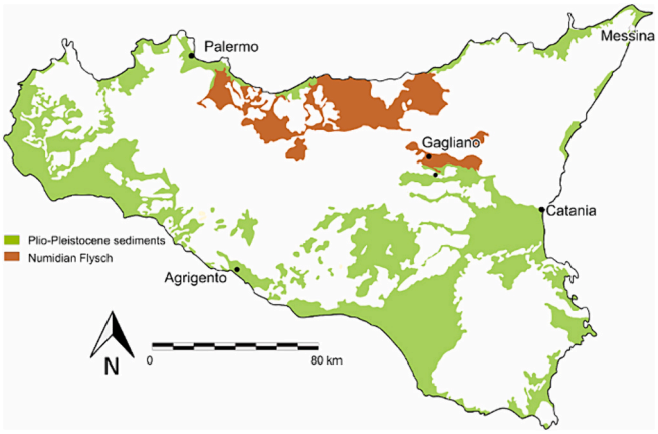

Fig. 1. Geological distribution of the two selected Sicilian clayey sediments.

understanding of both pre-activation treatments (thermal, mechanical, chemical), the factors influencing clay reactivity, the alkali activation process and the structural and mechanical properties of the final products. This opens up new opportunities for the exploitation of these resources to produce innovative materials by an alkali activation process (Ruiz-Santaquiteria et al., 2013; Tole et al., 2019; Khalifa et al., 2020). The aim of this paper is to investigate the potential of Sicilian clays, used as the sole precursor to produce two-part AAMs. From a geological point of view, Sicily (Italy) is characterized by a complex orogenic structure with the superposition of numerous units belonging to different paleodomains (Lentini and Carbone, 2014). Clay sediments belonging to this orogenic belt are widely distributed and present different mineralogical and chemical compositions (Barbera et al., 2009; Barbera et al., 2011). Furthermore, post orogenic neogenic and quaternary clay sediments are widely outcropping and are frequently characterized by high carbonate abundances (Di Grande and Giandinoto, 2002; Barone et al., 2019). In this context, the potential use of clay sediments in the production of binders and mortars through the alkaline activation process and their application in the construction and building sectors may be economically convenient due to their abundance and the reduction of transport distances. In this direction, the specific objective of this work is to explore the use of two Sicilian thermal treatment clays with different CaO contents (without <1%, and with ≈ 15% CaO), as possible precursors for the preparation of alkaline activated materials (AAMs).

2. Materials and methods

2.1. Clayey sediments selected

Two types of Sicilian clayey sediments were selected as potential raw materials to produce AAMs, as shown in Fig. 1:

i) brown-tobacco shale (Late Oligocene - Langhian) belonging to the Numidian Flysh Formation, which is widely exposed in north-central Sicily, Italy, hereafter referred to as **NU** (Barbera et al., 2014);
ii) grey-bluish marly clay (Late Pliocene – Early Pleistocene) of the Monte Narbone Formation, outcropping in southern Sicily, Italy, hereafter referred to as **PP**, (Di Grande and Giandinoto, 2002).

2.2. Characterization methods

The clayey precursors and the consolidated geopolymeric binders were characterized by using various analytical techniques. The mineralogical compositions were determined by powder X ray diffraction carried out with Rigaku Miniflex II with the following instrumental conditions: Cu Kα radiation; Ni filter; 2θ angle 5–65°, angular step of 0.01° 2θ; step time 5 s; divergence and antiscatter slits of 1° and receiving slit of 0.2 mm. Clay minerals were analyzed on oriented <2 μm grain size fraction scanned from 2θ to 35° 2 θ with a 0.02° 2 θ step size and a 4-s count time at 30 mA and 40 kV. The presence of swelling clay minerals was determined by treating samples with ethylene glycol at 60 °C for 12 h. (Moore and Reynolds, 1989). Semi-quantitative estimates of clay mineral abundances were obtained from the combination of pure mineral reflection profiles obtained using Newmod software. The best-fit analysis was performed by using the LINEST function in a home-made Excel macro (Barbera et al., 2011).

Chemical analyses were performed by X-ray fluorescence (XRF) spectrometry (Philips PW2404/00) on powder-pressed pellets; quantitative analysis was performed using a calibration line based on 45 international rock standards. The lower detection limits (LDL) were: SiO_2 = 1 wt%, TiO_2 = 0.01 wt%, Al_2O_3 = 0.1 wt%, Fe_2O_3 = 0.05 wt%, MnO = 0.01 wt%, MgO = 0.02 wt%, CaO = 0.05 wt%, Na_2O = 0.01 wt%, K_2O = 0.05 wt%, P_2O_5 = 0.01 wt%. The average relative standard deviations (RSD%) were <5%. Finally, the accuracy was evaluated using an international standard with a composition like the samples analyzed which is better than 2–5% for major elements.

FTIR-ATR spectra were obtained on the powdered samples using an Agilent Technologies Cary 630 FTIR infrared spectrometer. The data

Table 1
Detail of each formulation.

ID raw materials	ID	Powder (%)	NaOH % (4 M–6 M-8 M)	Na_2SiO_3 (%)	L/S ratio	IT after 7 day	IT after 28 days	Efflorescence after 28** days
PP	PP700-4 M	63.29	36.71	–	0.58	positive	positive	absent
PP	PP700-6 M	63.29	36.71	–	0.58	positive	positive	absent
PP	PP700-8 M	63.29	36.71	–	0.58	positive	positive	scarce
PP	PP700S-4 M	63.69	21.02	15.29	0.57	positive	positive	absent
PP	PP700S-6 M	63.69	21.02	15.29	0.57	positive	positive	absent
PP	PP700S-8 M	65.79	16.16	21.05	0.52	positive	positive	absent
NU	NU700-4 M	71.43	28.57	–	0.40	–	–	
NU	NU700-6 M	68.31	31.69	–	0.46	negative	positive	scarce
NU	NU700-8 M	68.49	31.51	–	0.46	positive	positive	scarce
NU	NU700S-4 M	71.43	8.57	20	0.40	positive	positive	scarce
NU	NU700S-6 M	68.31	15.30	16.39	0.46	positive	positive	scarce
NU	NU700S-8 M	71.43	8.57	20	0.40	positive	positive	absent

Table 2
Chemical composition (wt%) by pXRF of clay sediments: Plio-Pleisocenic clay (PP) and Numidian Clay (NU).

Materials	SiO_2	TiO_2	Al_2O_3	Fe_2O_3	MnO	MgO	CaO	Na_2O	K_2O	P_2O_5
NU	61.81	1.57	26.15	5.28	0.02	1.82	0.46	0.33	2.42	0.14
PP	57.41	0.80	15.18	5.31	0.05	2.81	14.88	1.10	2.27	0.18

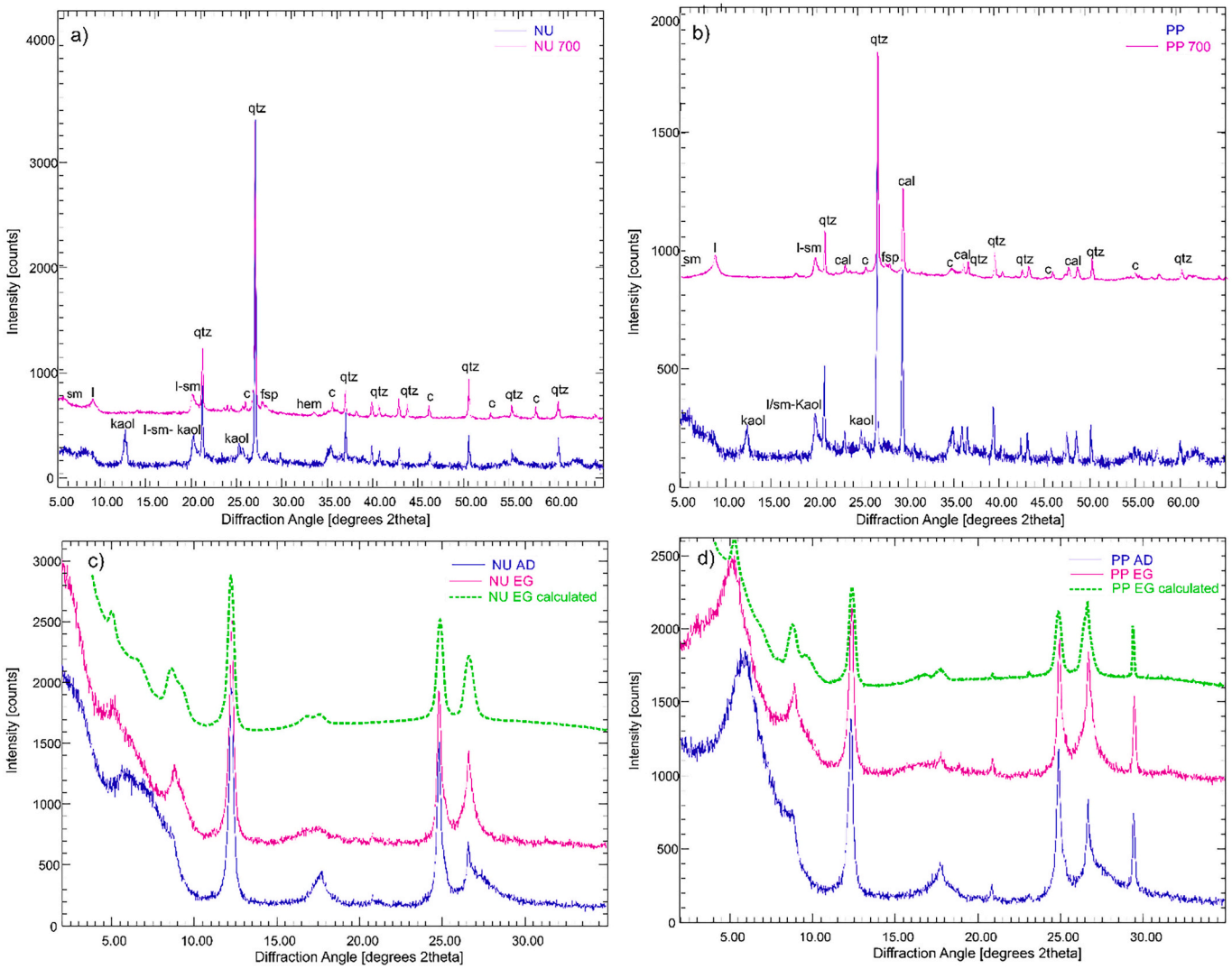

Fig. 2. XRPD patterns of Sicilian clayey: a) Numidian clay raw material and calcinated at 700 °C; b) Plio-Pleistocenic clay raw material as and calcinated at 700 °C; c) comparison between XRD patterns of Numidian clay raw material, Air-dried and glycolated; d) comparison between XRD patterns of Plio-Pleistocenic clay raw material, Air-dried and glycolated. In green the semi-quantitative esteem of the clay minerals abundance. qz = quartz; I = illite; sm = smectities; I-sm = Illite-smectite; kaol = kaolinite; fsp = feldspatoide; cal = calcite; crn = corundum.

were recorded at room temperature and the spectra were calculated by Fourier transformation of 64 interferometer scans in the wavenumber range between 650 and 4000 cm^{-1} with a resolution of 4 cm^{-1}.

Microstructural observations were made using a Field Emission Scanning Electron Microscope (SEM) (Zeiss FEG-SEM Supra 25 Microscope) equipped with an InLens detector coupled with an energy dispersive X-ray spectroscopy (EDX) microanalysis. Data were collected by focusing the e-beam on the sample at an energy of 25 kV and current of 0.2 nA. Measurements were made on gold-coated fragments.

The setting time of the fresh AAM paste was determined by using the Vicat Needle test according to ASTM C191, while the compressive strength was measured on the 2 × 2 × 2 cm^3 specimens after 28 days of curing using a 70-T1182 Uniframe (Controls) mechanical press according to NORM UNI EN 1926:20073. Measurements were carried out on six specimens for each sample, with a surface area 400 mm^2 and a speed of 2400 N/s.

2.3. AAMs preparation

The two selected clay materials were thermally treated at 700 °C for 3 h with the aim of dehydroxylizing the clay minerals and making them more reactive to alkaline attack (Provis et al., 2005; Kamseu et al., 2009; Lancellotti et al., 2013; Ferone et al., 2015; Wang et al., 2023a). The temperature of the thermal treatment was chosen on the basis of the thermogravimetric analysis reported in (Pulidori et al., 2022). Clays usually show three distinct stages of mass loss. The first, in the temperature range between 45° and 150 °C, can be attributed to hygroscopic loss of surface water. The other two, around 500 °C and 700 °C respectively, are related to the loss of structural hydration water and to decarbonation phenomena. In some cases, (Numidian clays, Plio-Pleistocenic clays), the presence of a small mass loss (about 1%) was observed around 250 °C, which could be due to the presence of organic matter. On average, Numidian clays show a first mass loss (3.2 wt%) at maximum temperature (T_{max}) ~ 60 °C followed by a second mass loss (5.2 wt%) at T_{max} ~ 500 °C. Plio-Pleiscocenic clays show the same two mass loss steps (3.1 wt% at T_{max} ~ 57 °C and 4.1 wt% at T_{max} ~ 500 °C) and additionally a stronger mass loss (8.1 wt%) at T_{max} ~ 718 °C due to calcite decarbonation (Pulidori et al., 2022). The activation solutions used for AAM synthesis are formed by 4, 6 or 8 M NaOH, as indicated in the sample name. In addition, sodium silicate with a molar ratio of SiO_2/Na_2O = 3 was added in variable proportions in the sample with S in the designation (Pacheco-Torgal et al., 2008). A liquid/solid ratio between

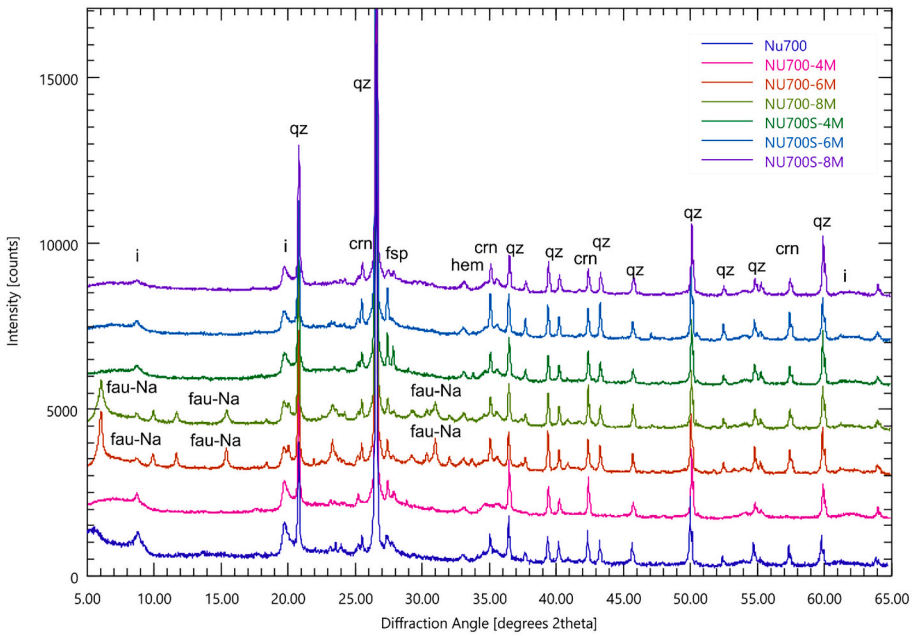

Fig. 3. XRPD patterns of Numidian clay raw material (NU700) and geopolymer sample (AAMs at 28 days) made with and without sodium silicate solution. qz = quartz; I = illite; fsp = feldspatoite; crn = corundum; dol = dolomite; hem = hematite; fau—Na: Na-faujasite.

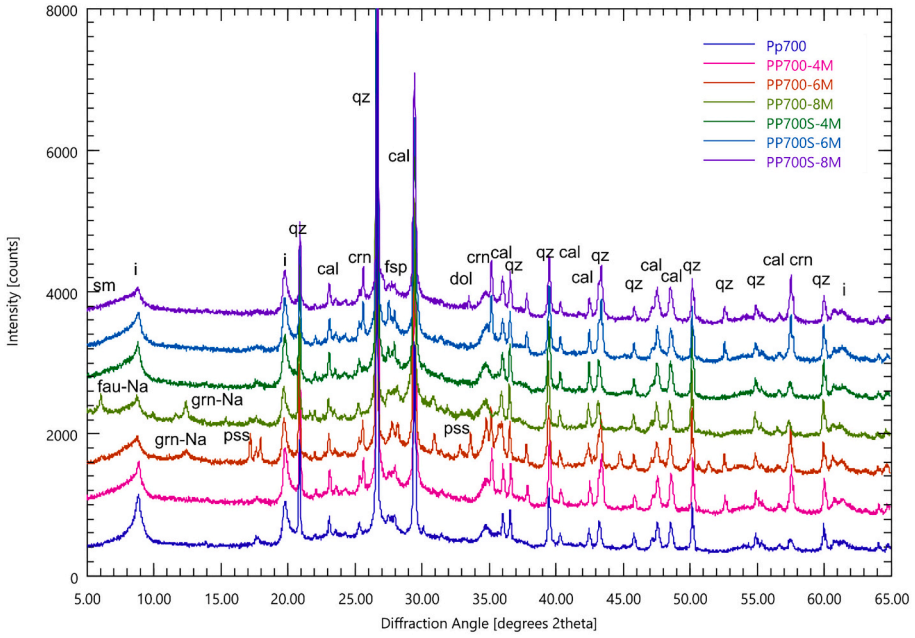

Fig. 4. XRPD patterns of Plio-Pleistocenic clay raw material (PP700) and geopolymer sample made with and without sodium silicate solution. qz = quartz; i = illite; fsp = feldspars; crn = corundum; dol = dolomite; fau-Na = Na-faujasite; cal = calcite; sm = smectities; grn-Na = garronite; Pss = pirssonite.

0.40 and 0.58 was used to obtain satisfactory workability. The pastes were mixed with a mechanical mixer for 5 min, then poured into 2 × 2 × 2 cm^3 molds and compacted with a mechanical vibrator for 60 s to facilitate the removal of air bubbles. All samples were cured at 85 °C for 20 h, to improve the alkaline reaction, and then at room temperature (22 ± 3 °C) for 28 days, keeping the humidity level always >90%. At the end of curing, the demoulded geopolymers appeared intact and without visible cracks. After the curing, a small amount of efflorescence was visible on some samples. All samples were tested for their chemical stability after 7 and 28 days through an Integrity Test (IT), which was performed by leaving the samples in water with a solid/liquid ratio of 1/10 for 24 h (Lancellotti et al., 2013). The IT was considered positive if the sample resisted without damage and the water remained clear. Table 1 shows the synthesis specification of each AAM, the result of the integrity test and the possible presence of efflorescence. Sample NU700-4 M did not harden after 28 days and therefore it did not perform the integrity test.

3. Results and discussion

3.1. Clayey precursors characterization

The mean and standard deviation of the chemical composition of the Numidian Flysh shale (calculated from 25 samples) and of the Plio-

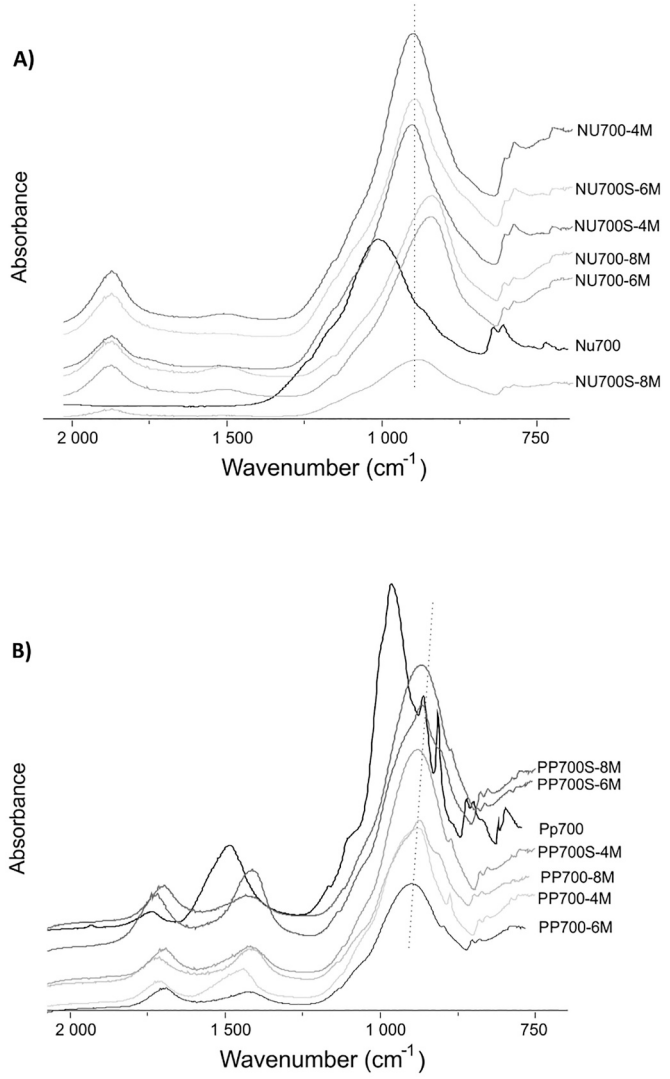

Fig. 5. ATR spectra: a) Numidian clay raw material (NU700) and relative geopolymers binders; b) Plio-Pleistocenic clay raw material (PP700) and relative geopolymers binders; The line indicates the aluminosilicate band of the geopolymer binders.

Pleistocenic marly clay (calculated from 23 samples) are given in Table 2, together with the two samples (NU and PP) used for the AAM production, sampled near the village of Gagliano and Agrigento respectively. The Numidian Flysh shales are high in SiO_2 and Al_2O_3 and low in CaO; the SiO_2/Al_2O_3 ratio is 3.78. The bulk mineralogical composition is characterized by high contents of clay minerals and quartz and low contents of feldspars. The NU semiquantitative XRD analysis of the <2 mm fraction showed the prevalence of R0 and R1 I/S mixed layer minerals (51%) and kaolinite (36%), (Fig. 2a and c).

The Plio-Pleistocene marly clays are characterized by a high CaO content, while $SiO_2 + Al_2O_3$ is 72.27 wt% and SiO_2/Al_2O_3 is 3.97. From mineralogical point of view, these clay sediments have high quartz and calcite contents, while in the <2 mm fraction smectite (57%) is the most abundant clay mineral followed by kaolinite (27%) and illite (16%) (Fig. 2b and d).

Regarding the X-ray diffraction patterns of the heat-treated clays, in NU700 the disappearance of kaolinite and the collapse of the I/S structure to the 10 Å illite can be observed (see Fig. 3). The same modification of clay minerals was observed in the heat-treated PP sample (PP700; Fig. 4), in which the calcite peaks also decrease in intensity (Ferone et al., 2015).

3.2. Consolidated geopolymers characterization

3.2.1. X-ray-powder diffraction (XRPD)

The mineralogical composition of the AAM samples obtained was determined out after 28 days of curing. Fig. 3 shows the mineralogical composition of the thermally treated Numidian clay (NU700) and the AAMs obtained with NaOH alone (4, 6 and 8 M) and with NaOH + sodium silicate. All the AAM samples show the same crystalline phases in the precursor, indicating that these phases are inert to alkaline activation. A new crystalline phase, Na-faujasite, is present in NU700-6 M and NU700-8 M.

AAM obtained from PP700 with NaOH only (PP700-4 M, PP700-6 M and PP700-8 M) and those obtained by adding sodium silicate PP700S-8 M, together with the clay raw material, calcined at 700 °C (PP700) are shown in Fig. 4. The mineralogical phases detected in the Plio-Pleistocenic raw materials (quartz, feldspars, calcite and illite) are still present in the geopolymeric binders obtained activated only with sodium hydroxide at different concentrations (4, 6 and 8 M). However, in the diffractometric pattern of the thermally treated sample (PP700), the phases resulting from calcite decomposition are not evident although a shoulder at 34.1 2 Θ and a halo at 18.3 2Θ could be attributed to portlandite, while a weak signal at 37.5 suggests the presence of lime. As reported in some cases in the literature, the absence of clear lime/portlandite peaks may be due to the low crystallinity of these phases or to the presence of an amorphous phase that masking the peaks (Mintsaev et al., 2022). Furthermore, zeolitic species are present in PP700-8 M (garronite and Na-faujasite) and in PP700-6 M (garronite only). In the latter, XRD shows the presence of pirssonite ($Na_2Ca(CO_3)_2{\cdot}2H_2O$).

3.2.2. Fourier Transform infrared spectroscopy in attenuated total reflection (FTIR-ATR)

The FTIR-ATR spectra of AAMs obtained from NU700 with NaOH alone (4, 6 and 8 M) and with NaOH + sodium silicate at 28 days are shown in (Fig. 5a-b). All geopolymer samples, with respect to the calcined clay, show bands in the interval around 2000 and 1650 cm^{-1}, respectively related to H-O-H bending vibrations of molecular water and O—H asymmetric stretching and bending vibrations respectively (Farmer, 1974b; Djobo et al., 2014; Clausi et al., 2016). Both bands, as well as the one attributed to O—H stretching, are broad and indicate a large disorder of hydroxyl groups and water molecules. All samples show another distinct peak in the range between 1080 and 1095 cm^{-1}, which are related to the aluminosilicate phase as quartz and k-feldspars. Peaks at 790–775 cm^{-1} and 691 cm^{-1}, related to the Si-O-Si bending vibration, are attributed to the presence of quartz in all samples analyzed(Farmer, 1974a; Lee and Van Deventer, 2003; Kaufhold et al., 2012). The evolution of the spectra is similar for both materials. In both cases, the reorganization of the network due to the geopolymerization reaction, (Rees et al., 2008; Prud'homme et al., 2013), is highlighted by the shift of the aluminosilicate bands, related to the asymmetric stretching of the Si-O-T bonds where T represents Al or Si in tetrahedral coordination, passing from 1002 cm^{-1} in the NU700 to 948–942 cm^{-1} in the products (Khan et al., 2015). Finally, samples made with Plio-Pleistocenic clay (PP700), Fig. 5b, show bands, in the range 1640–1391 cm^{-1} and 888–869 cm^{-1}, confirming the presence of $CaCO_3$, mainly in the form of calcite (García-Lodeiro et al., 2010). The attribution of these peaks is also confirmed by Diffuse Reflectance Infrared Fourier Transform spectroscopy (DRIFT) analysis, an innovative and non-invasive technique, as reported in (Caggiani et al., 2022).

3.2.3. Microstructural characteristics

SEM-EDS analyses were performed on all samples at different magnifications. In particular, the analysis of the structures was aimed at highlighting the differences between AAM with PP700 and NU700 precursors and cured by two modalities: 20 h at 85 °C and 28 days at room temperature.

Samples NU700-8 M (Fig. 6a) and NU700S-8 M (Fig. 6c) cured at

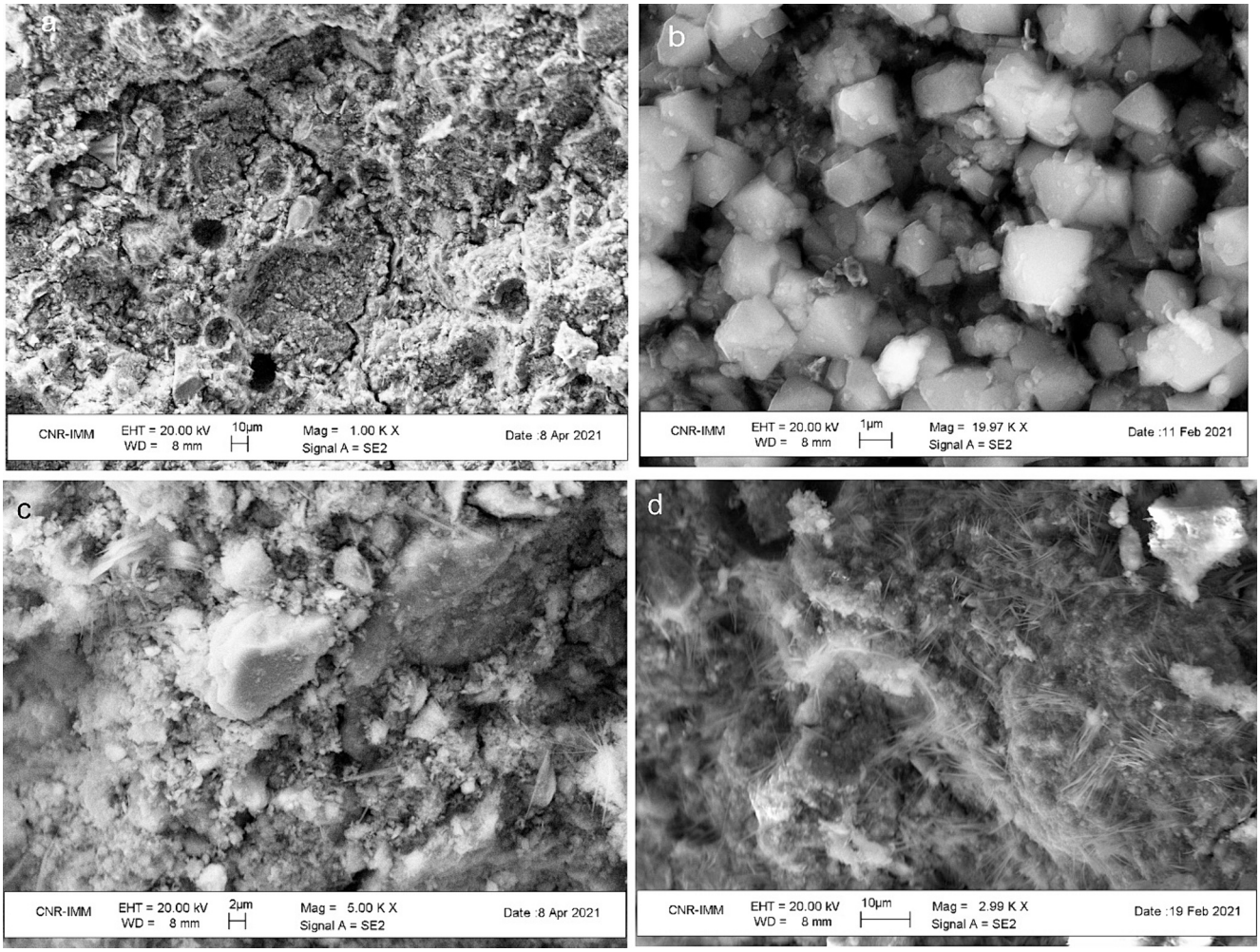

Fig. 6. Scanning electron microscopy micrographs of Numidian shale AAM: a) NU700-8 M cured at 85 °C for 20 h; b) NU700-8 M cured for 28 days at room temperature; c) NU700S-8 M cured at 85 °C for 20 h; d) NU700S-8 M cured at 85 °C for 20 h and for 28 days at room temperature.

85 °C for 20 h show similar microstructures characterized by granular not well compacted geopolymeric gel enveloping precursor particles with irregular morphologies. Both samples show micro-fractures and air bubbles. Furthermore, in sample NU700S-8 M, fibrous secondary structures (Fig. 6c) appear similar to those observed in geopolymers obtained with 8 M NaOH (Nath et al., 2016). The same samples, further cured for 28 days at room temperature, show peculiar features: in sample NU700-8 M (Fig. 6b), abundant zeolites crystallize, as also evidenced by the XRD pattern, while NU700S-8 M (Fig. 6d) is formed by a dense gel and abundant fibrous-like structure.

In Fig. 7 shows the main features of the PP700 geopolymers. With respect to the samples cured at 85 °C for 20 h, PP700-8 M (Fig. 7a) shows a spongy structure of the gel dispersed with zeolites while, in PP700S-8 M (Fig. 7c), the gel forms a compact smoothed structure. Curing for 28 days at room temperature results in a more developed structure with a well-structured gel in the PP700-8 M (Fig. 7b) and the formation of secondary fibrous structures (Fig. 7d).

The chemical analysis of the gel matrix obtained by SEM-EDS confirms the evolution of the alkali activated gel characterized by high SiO_2, Al_2O_3, Na_2O and variable CaO abundances. The classification of the AAM binders is carried out using the $CaO\text{-}SiO_2\text{-}Al_2O_3$ ternary diagram and the Al_2O_3/SiO_2 and CaO/SiO_2 binary diagrams (Fig. 8a-b). The gel composition of PP700 geopolymers is, mainly (N,C)-A-S-H and subordinately C-A-S-H type according to literature (Pardal et al., 2009; Garcia-Lodeiro et al., 2011; Bignozzi et al., 2013). Otherwise, geopolymeric binders made with Numidian clay (NU700) have gel compositions clustered in the N-A-S-H area.

3.2.4. *Compressive strength*

Fig. 9a and b show the values of compressive strength obtained for all the samples except for NU700-4 M, which did not consolidate. Analyses were carried out on six specimens for each sample after 20 h at 85 °C and after 28 days at room temperature.

AAM produced with Numidian Flysh shale (NU700) and only NaOH activation solution show low compressive strength after 20 h at 85 °C. The results deteriorate after 28 days at 22 °C demonstrating the absence of an extensive geopolymeric gel and the formation of abundant zeolites that break down the structure (see SEM images). On the contrary, the compressive strength of the samples activated with sodium silicate, on the contrary, increases after 28 days. NU700S-8 M recorded the highest resistance, reaching 17.89 MPa after 20 h and 44.50 MPa after 28 days, as shown in Fig. 9a. Geopolymers based on Plio-Pleistocenic marly clays (PP700) have good compressive strength values. In fact, among the samples activated with sodium hydroxide and cured at 85 °C for 20 h, only the Plio-Pleistocenic clay samples show good compressive strength values already after 20 h at 85 °C (23.31–25.95 MPa) except for the samples activated with 4 M NaOH. The data improve after 28 days of curing, reaching a maximum compressive strength of 29.84 MPa, Fig. 9b.

3.2.5. *Vicat Needle test*

The Vicat Needle test was carried out to determine the setting time of

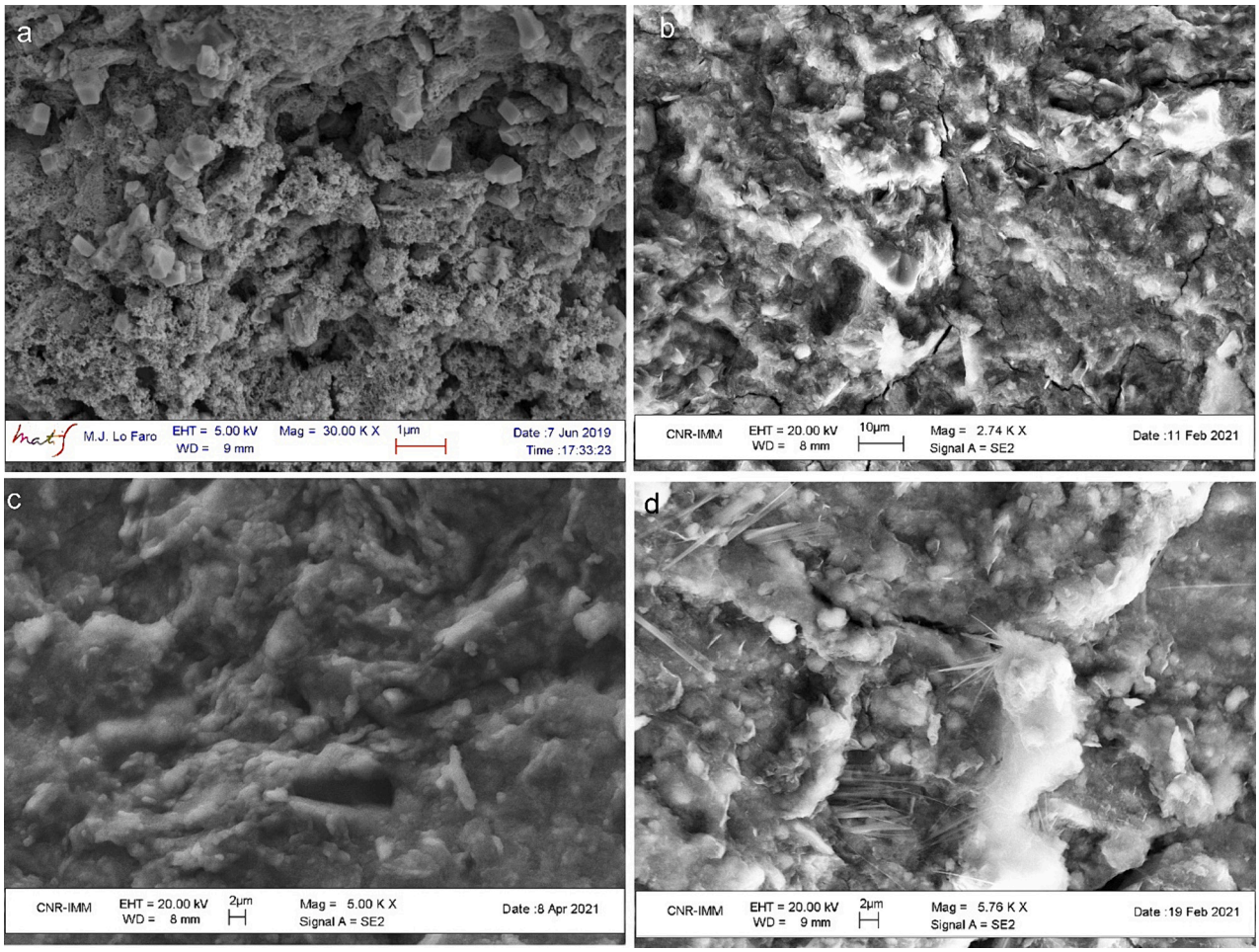

Fig. 7. Scanning electron microscopy micrographs of Plio-Pleistocenic (PP700) marly clays AAM: a) PP700-8 M cured at 85 °C for 20 h; b) PP700-8 M cured for 28 days at room temperature; c) PP700S-8 M cured at 85 °C for 20 h; d) PP700S-8 M cured for 20 h and for 28 days at room temperature.

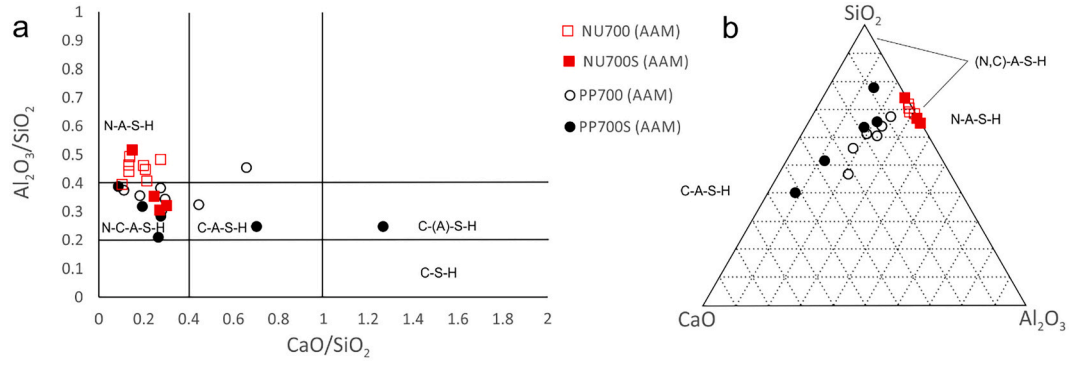

Fig. 8. Chemical composition of geopolymeric gel: a) Al_2O_3/SiO_2 vs. CaO/SiO_2; b) Ternary diagram Al_2O_3-SiO_2-CaO.

the geopolymer pastes. Unfortunately, for technical reasons, it was not possible to carry out the test during setting at 85 °C. However, it was decided to carry out the test on the freshly paste by measuring needle penetration at different times while everything was kept at room temperature. Thirty minutes after the mixing of the alkaline solution with the precursor, the needle was dropped for the first time and the depth reached was measured. The test was repeated every 15 min until a depth of <25 mm was reached. The behavior of the two samples geopolymers prepared with the two clay sediments is very different; in fact, PP700S-8 M reached a hardened state in <3 h, while sample NU700S-8 M needed about 48 h to reach a good hardness, as shown in Fig. 10a-b.

3.3. Discussion

The differences in the properties of the studied geopolymers reflect the diversity in the chemical and mineralogical composition of the Numidian and Plio-Pleistocenic clays. In this context, the abundance of calcite clayey sediments seems to play a key role not only in the mechanical properties but also in the formation of different gels. This effect is also dependent on the thermal treatment of the clay raw materials, which not only dehydroxylates the clay and makes the clay phases more reactive in the alkaline process, but also causes calcite decarbonation. The presence of lime in the precursor (PP700) causes a faster reaction

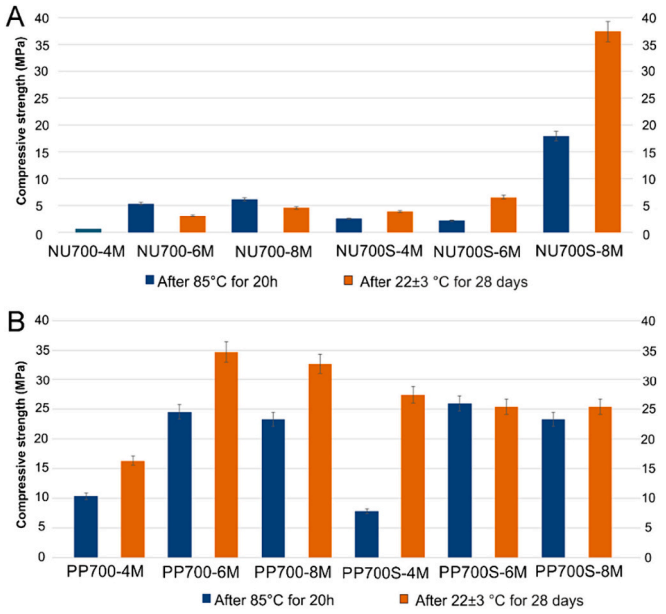

Fig. 9. Compressive strength values: a) Numidian Flysh based geopolymer binders; b) Plio-Pleistocenic based geopolymer binders. The bar indicates the error on the measurement accuracy.

and a higher mechanical strength than in the NU700 AAM. Regarding the newly formed gels, geopolymers based on the low CaO Numidian Flysh are characterized by an N-A-S-H gel while geopolymers based on the high CaO Plio-Pleistocenic are characterized by an (N, C)-A-S-H and C-A-S-H gel.

In this context, the composition of the activation solutions and the curing methods play a different role in determining the mechanical properties for the two clay sediments precursors. For Numidian Flysch shale (NU700 without CaO), the formation of a geopolymeric gel with good mechanical resistance is only guaranteed by sodium silicate combined with high molarity sodium hydroxide. Furthermore, the SEM images show the formation of a well-developed gel, especially after 28 days of curing at room temperature.

On the contrary, Plio-Pleistocenic clay sediments (NU700 with ~15% CaO) produce geopolymers with good mechanical properties even with only NaOH in the activation solution. The molarity of the sodium hydroxide plays a minor role, since an acceptable compressive strength is obtained already at 4 M. These observations are explained by the formation of a C-A-S-H gel, which contributes to the mechanical properties of the geopolymers, as shown by SEM images and EDS analysis. This aspect is more evident in all the samples cured at room temperature for 28 days than in those cured at 85 °C for 20 h.

Noteworthy is the formation of zeolitic phases in the geopolymers of both clayey precursors when the activation solution is NaOH 6 - 8 M. The formation of these new phases negatively affected the mechanical strength value of NU700-6 M and NU700-8 M interrupting the continuity of the geopolymeric gel (Longhi et al., 2019), while for PP700-6 M and PP800-8 M the presence of zeolites does not significantly contrast the compact structure.

4. Conclusions

To summarize, the most important results are hereafter listed:

- The diversity in chemical and mineralogical composition of the Numidian and Plio-Pleistocene clays resulted in different characteristics of the geopolymers studied.
- Geopolymerization occurs in all the formulations tested, except for sample NU700-4 M, which was cured at 22 °C for 28 d, at different molarities and proportions of the alkaline solution and at different curing temperatures.
- The gel appears as a multicomponent system dominated by an (N, C)-A-S-H composition, also showing N-A-S-H (mainly for samples made with Numidian clay) or C-A-S-H (mainly for samples made with Plio-Pleistocenic clay) areas, in which minor amounts of zeolites and other mineral phases have been found as secondary products.
- Overall, the mechanical strength increases with increasing molarities of the NaOH used, when sodium silicate is added to the mixture and as a function of the curing time.
- In conclusion, this work shows that clays thermally treated at 700 °C can be used as precursors for alkaline cements due to the modification of clay minerals and, if present, the calcite decarbonation. In particular, CaO plays an important role in the consolidation mechanism, making the calcite-bearing precursor more suitable for AAM production.

CRediT authorship contribution statement

Antonio Stroscio: Writing – original draft, Methodology, Investigation, Data curation, Conceptualization. **Germana Barone:** Writing – review & editing, Validation, Supervision, Project administration, Methodology, Funding acquisition, Conceptualization. **Ana Fernàndez-Jimenez:** Writing – review & editing, Methodology. **Isabella Lancellotti:** Writing – review & editing, Methodology. **Cristina Leonelli:** Writing – review & editing, Methodology. **Paolo Mazzoleni:** Writing – review & editing, Validation, Supervision, Project administration, Methodology, Funding acquisition, Conceptualization.

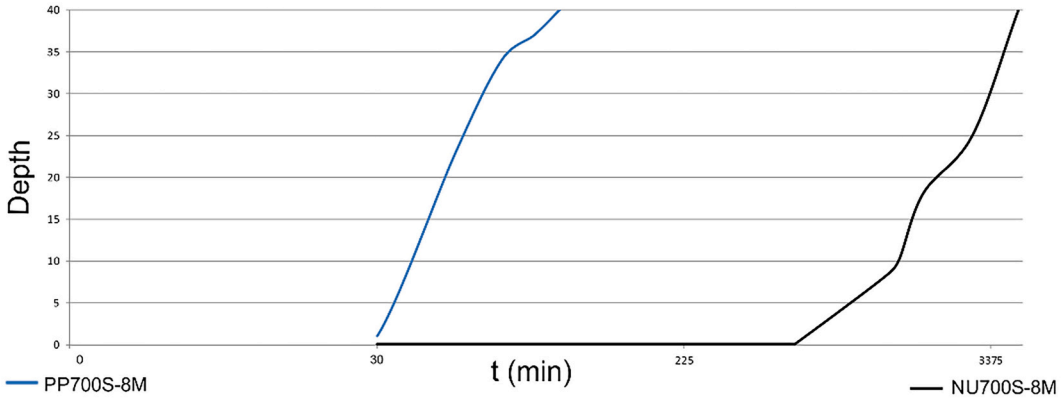

Fig. 10. Vicat Needle test: needle penetration depth on PP700S-8 M and NU700S-8 M samples.

Declaration of competing interest

The authors declare that they have no known competing financial interests or personal relationships that could have appeared to influence the work reported in this paper.

Data availability

The data that has been used is confidential.

Acknowledgements

This work was supported by the Advanced Green Materials for Cultural Heritage (AGM for CuHe) project (PNR fund with code: ARS01_00697; CUP E66C18000380005) and by Ph.D Grant PO FSE Sicilia 2020 (CUP E64F18000430009).

References

Barbera, G., Lo Giudice, A., Mazzoleni, P., Pappalardo, A., 2009. Combined statistical and petrological analysis of provenance and diagenetic history of mudrocks: application to Alpine Tethydes shales (Sicily, Italy). Sediment. Geol. 213.

Barbera, G., Critelli, S., Mazzoleni, P., 2011. Petrology and geochemistry of cretaceous sedimentary rocks of the Monte Soro Unit (Sicily, Italy): constraints on weathering, diagenesis, and provenance. J. Geol. 119, 51–68.

Barbera, G., Barone, G., Mazzoleni, P., Puglisi, D., Khozyem, H.M., Osama, M., 2014. Mineralogy and geochemistry of the Numidian formation Central-Northern Sicily: intra-formation variability and provenance evaluation. Ital. J. Geosci. 133, 13–26.

Barone, G., Mazzoleni, P., Spagnolo, G.V., Raineri, S., 2019. Artificial neural network for the provenance study of archaeological ceramics using clay sediment database. J. Cult. Herit. 38.

Barone, G., Caggiani, M.C., Coccato, A., Finocchiaro, C., Fugazzotto, M., Lanzafame, G., Occhipinti, R., Stroscio, A., Mazzoleni, P., 2020. Geopolymer production for conservation-restoration using Sicilian raw materials: feasibility studies. In: Functional Materials for Cultural Heritage (Fun4Heritage).

Benito, P., Leonelli, C., Medri, V., Vaccari, A., 2013. Geopolymers: A new and smart way for a sustainable development. Appl. Clay Sci., 73 (1), 1.

Bignozzi, M.C., Manzi, S., Lancellotti, I., Kamseu, E., Barbieri, L., Leonelli, C., 2013. Mix-design and characterization of alkali activated materials based on metakaolin and ladle slag. Appl. Clay Sci., 73, 78–85.

Caggiani, M.C., Occhipinti, R., Finocchiaro, C., Fugazzotto, M., Stroscio, A., Mazzoleni, P., Barone, G., 2022. Diffuse reflectance infrared Fourier Transform spectroscopy (DRIFTS) as a potential on site tool to test geopolymerization reaction. Talanta 250.

Christophliemk, M.P., Pikkarainen, A.T., Heponiemi, A., Tuomikoski, S., Runtti, H., Hu, T., Kantola, A.M., Lassi, U., 2022. Preparation and characterization of porous and stable sodium- and potassium-based alkali activated material (AAM). Appl. Clay Sci. 230, 106697.

Clausi, M., Tarantino, S.C., Magnani, L.L., Riccardi, M.P., Tedeschi, C., Zema, M., 2016. Metakaolin as a precursor of materials for applications in cultural heritage: geopolymer-based mortars with ornamental stone aggregates. Appl. Clay Sci. 132–133, 589–599. Elsevier B.V.

Davidovits, J., 1991. Geopolymers: inorganic polymeric new matrials. J. Therm. Anal. Calorim., 37 (8), 1633–1656.

Di Grande, A., Giandinoto, V., 2002. Plio-Pleistocene sedimentary facies and their evolution in Centre-South-Eastern Sicily: a working hypothesis. In: EGU Stephan Mueller Special Publication Series, 1, pp. 211–221.

Djobo, J.N.Y., Tchadjié, L.N., Tchakoute, H.K., Kenne, B.B.D., Elimbi, A., Njopwouo, D., 2014. Synthesis of geopolymer composites from a mixture of volcanic scoria and metakaolin. J Asian Ceram. Soc. 2 (4), 387–398.

Farmer, V.C., 1974a. Infrared Spectra of Minerals. Mineralogical Society.

The infrared spectra of minerals. In: Farmer, V.C. (Ed.), 1974b. Mineralogical Society of Great Britain and Ireland, Londan.

Fernández-Jiménez, A., Palomo, A., 2009. Nanostructure/microstructure of fly ash geopolymers. In: Geopolymers: Structures, Processing, Properties and Industrial Applications, pp. 89–117.

Ferone, C., Liguori, B., Capasso, I., Colangelo, F., Cioffi, R., Cappelletto, E., Di Maggio, R., 2015. Thermally treated clay sediments as geopolymer source material. Appl. Clay Sci. 107, 195–204.

García-Lodeiro, I., Fernández-Jiménez, A., Palomo, A., Macphee, D.E., 2010. Effect of calcium additions on N-A-S-H cementitious gels. J. Am. Ceram. Soc. 93 (7), 1934–1940.

Garcia-Lodeiro, I., Palomo, A., Fernández-Jiménez, A., Macphee, D.E., 2011. Compatibility studies between NASH and CASH gels. Study in the ternary diagram Na_2O-CaO-Al_2O_3-SiO_2-H_2O. Cem. Concr. Res. 41 (9), 923–931.

Juenger, M.C.G., Winnefeld, F., Provis, J.L., Ideker, J.H., 2011. Advances in alternative cementitious binders. Cem. Concr. Res. 41, 1232–1243.

Kamseu, E., Leonelli, C., Perera, D.S., Melo, U.C., Lemougna, P.N., 2009. Investigation of volcanic ash based geopolymers as potential building materials. Int. Ceram. Rev. 58, 136–140.

Kang, X., Li, Y., Li, W., Zhou, Y., Cui, J., Cai, B., Zi, Y., Fang, J., 2023. Synthesis and characterization of sustainable eco-friendly alkali-activated high-content iron ore tailing bricks. Buildings 1–20.

Kaufhold, S., Hein, M., Dohrmann, R., Ufer, K., 2012. Quantification of the mineralogical composition of clays using FTIR spectroscopy. Vib. Spectrosc. 59, 29–39. Elsevier B. V.

Khalifa, A.Z., Cizer, Ö., Pontikes, Y., Heath, A., Patureau, P., Bernal, S.A., Marsh, A.T.M., 2020. Advances in alkali-activation of clay minerals. Cem. Concr. Res. 132, 106050. Elsevier.

Khan, M.I., Azizlin, K., Sufian, S., Man, Z., 2015. Sodium silicate-free geopolymers as coating materials: Effects of Na/Al and water/solid ratios on adhesion strength. Ceramics. International 41, 2794–2805.

Lancellotti, I., Catauro, M., Ponzoni, C., Bollino, F., Leonelli, C., 2013. Inorganic polymers from alkali activation of metakaolin: effect of setting and curing on structure. J. Solid State Chem. 200, 341–348.

Lee, W.K.W., Van Deventer, J.S.J., 2003. Use of infrared spectroscopy to study geopolymerization of heterogeneous amorphous aluminosilicates. Langmuir 19, 8726–8734.

Lentini, F., Carbone, S., 2014. Geologia della Sicilia. Con i contributi di S. Branca (vulcanico), A. Messina (basamenti cristallini). In: Ispra, Mem. Descr. Carta geol. D'it, xcv, pp. 7–414.

Liang, G., Liu, T., Li, H., Dong, B., Shi, T., 2022. A novel synthesis of lightweight and high-strength green geopolymer foamed material by rice husk ash and ground-granulated blast-furnace slag. Resour. Conserv. Recycl. 176, 105922. Elsevier B.V.

Longhi, M.A., Zhang, Z., Rodríguez, E.D., Kirchheim, A.P., Wang, H., 2019. Efflorescence of alkali-activated cements (geopolymers) and the impacts on material structures: a critical analysis. Front. Mater. 6, 1–13.

Mintsaev, M., Murtazaev, S.A., Salamanova, M., Bataev, D., Saidumov, M., Murtazaev, I., Fediuk, R., 2022. Structural formation of alkali-activated materials based on thermally treated Marl and Na_2SiO_3. Materials 15, 1–14.

Moore, D.M., Reynolds, J., 1989. X-Ray Diffraction and the Identification and Analysis of Clay Minerals, second edition. Oxford University press.

Nath, S.K., Maitra, S., Mukherjee, S., Kumar, S., 2016. Microstructural and morphological evolution of fly ash based geopolymers. Constr. Build. Mater. 111, 758–765. Elsevier Ltd.

Occhipinti, R., Stroscio, A., Finocchiaro, C., Fugazzotto, M., Leonelli, C., José Lo Faro, M., Megna, B., Barone, G., Mazzoleni, P., 2020. Alkali activated materials using pumice from the Aeolian Islands (Sicily, Italy) and their potentiality for cultural heritage applications: preliminary study. Constr. Build. Mater. 259, 120391. Elsevier Ltd.

Oh, J.E., Jun, Y., Jeong, Y., 2014. Characterization of geopolymers from compositionally and physically different class F fly ashes. Cem. Concr. Compos. 50, 16–26. Elsevier Ltd.

Pacheco-Torgal, F., Castro-Gomes, J., S.J, 2008. Alkali-activated binders: a review: part 1. Historical background, terminology, reaction mechanisms and hydration products. Constr. Build. Mater. 22, 1305–1314.

Pardal, X., Pochard, I., Nonat, A., 2009. Experimental study of Si-Al substitution in calcium-silicate-hydrate (C-S-H) prepared under equilibrium conditions. Cem. Concr. Res. 39, 637–643. Elsevier Ltd.

Provis, J.L., 2018. Alkali-activated materials. Cem. Concr. Res. 114, 40–48.

Provis, J.L., Duxson, P., van Deventer, J.S.J., Lukey, G.C., 2005. The role of mathematical modelling and gel chemistry in advancing geopolymer technology. Chem. Eng. Res. Des. 83, 853–860.

Prud'homme, E., Autef, A., Essaidi, N., Michaud, P., Samet, B., Joussein, E., Rossignol, S., 2013. Defining existence domains in geopolymers through their physicochemical properties. Appl. Clay Sci., 73, 26–34.

Pulidori, E., Lluveras-Tenorio, A., Carosi, R., Bernazzani, L., Duce, C., Pagnotta, S., Lezzerini, M., Barone, G., Mazzoleni, P., Tiné, M.R., 2022. Building geopolymers for CuHe part I: thermal properties of raw materials as precursors for geopolymers. J. Therm. Anal. Calorim. 147, 5323–5335.

Qin, Y., Qu, C., Ma, C., Zhou, L., 2022. One-part alkali-activated materials: state of the art and perspectives. Polymers 14, 5046.

Rees, C.A., Provis, J.L., Lukey, C.G., Van Deventer J.S.J., 2008. The mechanism of geopolymer gel formation investigated through seeded nucleation. Colloids and Surfaces A: Physicochem. Eng. Aspects 318 (2008) 97–105.

Ruiz-Santaquiteria, C., Fernández-Jiménez, A., Skibsted, J., Palomo, A., 2013. Clay reactivity: production of alkali activated cements. Appl. Clay Sci. 73, 11–16. Elsevier B.V.

Schmücker, M., MacKenzie, K.J.D., 2005. Microstructure of sodium polysialate siloxo geopolymer. Ceram. Int. 31, 433–437.

Tchakouté, H.K., Melele, S.J.K., Djamen, A.T., Cyriaque R. K., Kamseu E., Charles N.P. N., Leonelli, C., Rüscher, C.H., 2020. Microstructural and mechanical properties of poly (sialate-siloxo) networks obtained using metakaolins from kaolin and halloysite as aluminosilicate sources: A comparative study, Appl. Clay Sci., 186,105448.

Tole, I., Habermehl-Cwirzen, K., Cwirzen, A., 2019. Mechanochemical activation of natural clay minerals: an alternative to produce sustainable cementitious binders – review. Mineral. Petrol. 113, 449–462.

Van Deventer, J.S.J., Provis, J.L., Duxson, P., Brice, D.G., 2010. Chemical research and climate change as drivers in the commercial adoption of alkali activated materials. Waste Biomass Valoriz. 1.

Vasic, M.V., Terzic, A., Radovanovic, Z., Radojevic, Z., Warr, L.N., 2022. Alkali-activated geopolymerization of a low illitic raw clay and waste brick mixture. An alternative to traditional ceramics. Appl. Clay Sci. 218, 106410.

Wang, W., Gan, Y., Kang, X., 2021. Synthesis and characterization of sustainable eco-friendly unburned bricks from slate tailings. J. Mater. Res. Technol. 14, 1697–1708. Elsevier Ltd.

Wang, S., Gainey, L., Mackinnon, I.D.R., Allen, C., Gu, Y., Xi, Y., 2023a. Thermal behaviors of clay minerals as key components and additives for fired brick properties: a review. J. Build. Eng. 66, 105802. Elsevier Ltd.
Wang, W., Zhong, Z., Kang, X., Ma, X., 2023b. Physico-mechanical properties and micromorphological characteristics of graphene oxide reinforced geopolymer foam concrete. J. Build. Eng. 72, 106732. Elsevier Ltd.
Žibret, L., Wisniewski, W., Horvat, B., Božič, M., Gregorc, B., Ducman, V., 2023. Clay rich river sediments calcined into precursors for alkali activated materials. Appl. Clay Sci. 234, 106848.